FULL PAPER

Macromolecular
Chemistry and Physic
www.mcp-journal.d

Check for
updates

Micelles with a Loose Core Self-Assembled from Coil-g-Rod Graft Copolymers Displaying High Drug Loading Capacity

Qijing Huang, Zhanwen Xu, Chunhua Cai, and Jiaping Lin**

High drug loading capacity is one of the critical demands of micellar drug-delivery vehicles; however, it is a challenging work. Herein, it is demonstrated that micelles self-assembled from poly(ethylene glycol)-*graft*-poly(γ-benzyl-ʟ-glutamate) (PEG-*g*-PBLG) coil-*g*-rod graft copolymers display high drug-loading capacity for doxorubicin (DOX) model drugs. As revealed by a combination study of experiments and dissipative particle dynamics simulations, the high drug-loading capacity of the micelles is related to the loose core structure of the micelles. In these micelles, the hydrophobic PBLG grafts randomly disperse in the micelle core due to their rigid nature and the coil-*g*-rod topology of the graft copolymers, which results in a loose core of the micelles. The structure of the graft copolymer, including the length of rod grafts, the length of coil backbone, and the grafting ratio of the rod grafts affecting the arrangement of the rod grafts in the micelle core has influence on the drug-loading capacity of the micelles. Besides, the strong π–π stacking interaction between graft copolymers and DOX also plays an important part in achieving high drug-loading capacity. In vitro studies reveal that these drug-loaded micelles show good biocompatibility, and the DOX can be gradually released from the micelles.

1. Introduction

Block and graft copolymers are capable of self-assembling into core–shell micelles in solutions.[1–5] The hydrophilic shell endows high stability of the micelles in aqueous solution, and the hydrophobic core of the micelles acts as reservoir of various hydrophobic species.[6–8] In the past decades, polymeric micelles have been comprehensively investigated as drug delivery carriers, which can improve the solubility of hydrophobic drugs, prolong their blood circulation, and reduce their side effect.[7,9–13] Especially the micelles prepared from biocompatible polymers, such as polypeptide-based copolymers, have attracted special interest in this field.[14–16]

High drug-loading content (DLC) is one of the key demands of the drug delivery systems. However, in most cases, the DLC is relatively low, typically on the level of 10 wt%, which is one of the obstacles impeding their successful translation to clinic.[17–20] It is still a challenge to achieve high drug-loading contents in convenient ways for most polymeric micelles.[18,19] Enhancing the attraction between the core-forming polymers and the drugs is a common and effective way to increase the DLC of the micelles. It is reported that the drug-loading capacity of the micelles can be improved by the introduction of physical interactions such as π–π stacking interaction, hydrogen bonding, and electrostatic interactions between polymers and drugs.[21–24] However, this route lacks universal validity since special chemical modifications of the polymers are usually needed. On the other hand, the low drug-loading capacity of the micelles could be related to their compact core, since the hydrophobic core-forming polymers are usually densely packed in the core region. As a matter of fact, hollow micro-particles usually show high DLCs. The large cavity inside the hollow micro-particles can provide enough space for encapsulating drugs and induce high drug-loading contents.[25] However, the preparation of the hollow micro-particles is a complex process.[25–27] Therefore, it is conceived that the micelles with a loose core could be promising in achieving high DLCs; however, there is no direct work referring this topic up to now.

In this work, we report that micelles with remarkably high DLCs are prepared by the self-assembly of poly(ethylene glycol)-*graft*-poly(γ-benzyl-ʟ-glutamate) (PEG-*g*-PBLG) coil-*g*-rod copolymers using doxorubicin (DOX) as a model drug (**Scheme 1**). These graft copolymers were synthesized using a commercially obtained PEG-*g*-NH$_2$ as initiator, in which the degree of polymerization (DP) of the PEG backbone is 110, and the substitution number of the amino groups is 11. The typical graft copolymer used in this work is PEG$_{110}$-*g*-(PBLG$_{28}$)$_{11}$ (the subscripts "110" and "28" denote the degree of polymerization of PEG and PBLG segments, respectively, and the subscript "11" denotes the grafting number of the PBLG side chains). For these graft copolymers, the PEG backbone is a hydrophilic coil polymer and forms the shell of the micelle, and the PBLG side chain is a hydrophobic rigid polymer and forms

Q. Huang, Dr. Z. Xu, Prof. C. Cai, Prof. J. Lin
Shanghai Key Laboratory of Advanced Polymeric Materials
Key Laboratory for Ultrafine Materials of Ministry of Education
School of Materials Science and Engineering
East China University of Science and Technology
Shanghai 200237, China
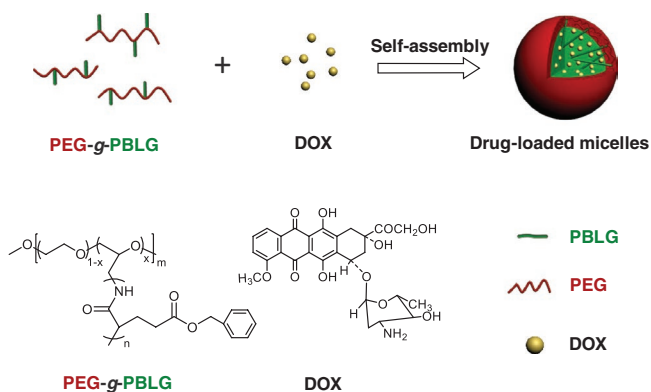E-mail: caichunhua@ecust.edu.cn; jlin@ecust.edu.cn

The ORCID identification number(s) for the author(s) of this article can be found under https://doi.org/10.1002/macp.202000121.

Scheme 1. Scheme for the preparation of the drug-loaded micelles, and the structures of the PEG-*g*-PBLG graft copolymer and DOX.

the core of the micelle. The structures of the blank micelles and drug-loaded micelles were explored by a combination of experiment and simulation studies. The loose core structure of the micelles generated from the coil-*g*-rod topology of the copolymers is proved to contribute to the high drug-loading capacity. The in vitro drug release behavior and cytotoxicity of drug-loaded micelles were also studied.

2. Experimental Section

2.1. Materials

Polyethylene glycol-*graft*-amino (PEG-*g*-NH$_2$, M_n = 5000, PDI = 1.03, DP of the PEG backbone is 110, and the grafting ratio of the amino groups is 10%) was purchased from SINOPEG Inc. Polyethylene glycol monomethyl ether (mPEG-OH) (M_n = 750) and α-methoxy-ω-amino poly(ethylene glycol) (mPEG-NH$_2$) (M_n = 2000) were purchased from Sigma Inc. γ-Benzyl-L-glutamate-*N*-carboxyanhydride (BLG-NCA) was synthesized according to literature.[28] The details of the synthesis and characterizations are provided in Supporting Information. Doxorubicin hydrochloride (DOX·HCl) was purchased from Adamas-beta. Deionized water was prepared in a Millipore Super-Q Plus Water System to a level of 18.2 MΩ cm resistance. All the solvents and other reagents were of analytical grade and used without further purification.

2.2. Synthesis of Copolymers

2.2.1. Synthesis of PEG-*g*-PBLG Graft Copolymers and poly(γ-benzyl-L-glutamate)-block-poly(ethylene glycol) (PBLG-*b*-PEG) Block Copolymers

PEG-*g*-PBLG graft copolymers and PBLG-*b*-PEG block copolymers were synthesized by ring-opening polymerization of BLG-NCA initiated by PEG-*g*-NH$_2$ and mPEG-NH$_2$, respectively. The molecular weight of the copolymers was adjusted by varying the feed molar ratio of the BLG-NCA to the macroinitiators. The reactions were performed in anhydrous 1,4-dioxane at 15 °C. After 3 days, the viscous reaction mixture was poured into a

large volume of anhydrous ethanol. The precipitated product was dried under vacuum and then purified twice by repeated precipitation from a chloroform solution into a large volume of anhydrous methanol. After being dried under vacuum, a white powder was obtained.

2.2.2. Synthesis of poly(γ-benzyl-L-glutamate)-graft-poly(ethylene glycol) (PBLG-g-PEG) Graft Copolymers

First, PBLG homopolymers were synthesized by ring-opening polymerization of BLG-NCA initiated by trimethylamine in anhydrous 1,4-dioxane.[3] PBLG-*g*-PEG graft copolymers were then prepared by ester exchange reaction of PBLG homopolymers with mPEG-OH.[29] The feed molar ratio of mPEG-OH to BLG units was 1/1 (i.e., n$_{PEG}$/n$_{BLG}$, 1/1), and the reaction was performed at 55 °C in 1,2-dichloroethane with *p*-toluenesulfonic acid as a catalyst. After reacting for 1 h, the reaction mixture was precipitated into a large volume of anhydrous methanol. The product was purified twice by repeated precipitation from a chloroform solution into a large volume of anhydrous methanol and finally dried under vacuum.

Table 1 shows the structural characteristics of the typical PEG-*g*-PBLG graft copolymers, PBLG-*b*-PEG block copolymers, and PBLG-*g*-PEG graft copolymers used in this work.

2.3. Preparation of Drug-Loaded Micelles

The preparation of the drug-loaded micelles was as follows: First, the PEG-*g*-PBLG graft copolymers and DOX were separately dissolved in *N,N′*-dimethylformamide (DMF). The concentration was 0.3 g L^{-1} for all the solutions. Mixture solutions of copolymer and DOX with various DOX weight fractions (f_{DOX}) were prepared by mixing these two stock solutions. The total concentration of the solutes (polymers and DOX) in the solutions is 0.3 g L^{-1}. Then, water (1 mL) was slowly added to PEG-*g*-PBLG/DOX mixture solutions (2 mL) under stirring. After dialyzing against water for 3 days, the aqueous solutions of the drug-loaded micelles were prepared.
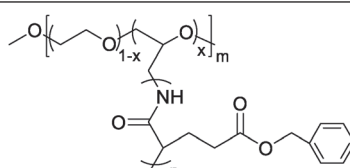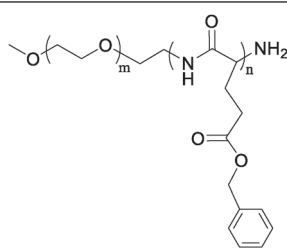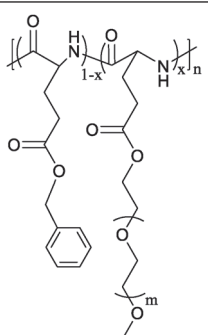
2.4. Determination of Drug-Loading Content of the Micelles

Drug-loaded micelle solutions (1 mL) were added into DMF (4 mL) and shaken overnight to break up the micelles and release the DOX. The solutions were then analyzed by a UV–vis spectrometer (UV-2550, SHIMADZU). The absorbance of solutions at 485 nm was recorded where DOX had a characteristic absorbance. By comparing the absorbance with the standard curve generated from DMF/H$_2$O (v/v = 4/1) mixture with various DOX concentrations ranging from 2–15 μg mL^{-1}, the weight of DOX loaded in micelles was obtained.

2.5. In Vitro Drug Release Study

Micelle solution (5 mL) was transferred to dialysis tube and immersed into buffer solutions of pH = 5.5 and 7.4. Then, the

Table 1. Characteristics of the copolymers.

Sample	PEG-*g*-PBLG	PBLG-*b*-PEG	PBLG-*g*-PEG
Structure			
DP$_{PBLG}$	28	132	548
DP$_{PEG}$	110	45	17
GR (mol%)	10	/	1.4
Đ	1.38	1.24	1.15

GR, grafting ratio of the graft copolymer.

samples were laid in shaker at 90 ± 4 rpm, at 37 °C. The buffer solutions were sampled and replaced by fresh solutions at regular intervals. The DOX contents in the buffer solutions were determined according to the standard curves at different pH values.

2.6. Cytotoxicity Measurements

The relative cytotoxicity of drug-loaded micelles against NIH/3T3 cells was estimated by the tetrazolium salt (MTT) assay. NIH/3T3 cells were seeded into 96-well plates at a density of 5×10^5 cells per well in Dulbecco's modified Eagle's medium (DMEM). After culturing for 2 days, the cell culture medium was replaced by medium (100 μL) containing blank micelles, free DOX, and drug-loaded micelles solutions. After incubating for another 48 h, the culture medium was removed and the wells were washed with PBS solutions twice, and then 0.5 g L^{-1} MTT solution in PBS (100 μL) was added into each well. After further incubation for 4 h at 37 °C, the medium was removed and dimethyl sulfoxide DMSO (100 μL) was added. Finally, the absorbance at 570 nm was measured using a UV–vis spectrometer. The cell viability was calculated as a percentage of absorbance relative to control cells. Each experiment was carried out triplicate.

2.7. Simulation Parameters

All the dissipative particle dynamics (DPD) simulations were performed in a $32 \times 32 \times 32$ simulation box, where NVT ensemble and periodic boundary conditions were adopted. In the simulation, more than 1×10^7 DPD steps were performed so that the computing time was long enough for the system to achieve an equilibrium state. The interaction parameters between different types of beads are shown in **Table 2**. The R, C, D, and S in the table are corresponding to the rod beads, coil beads, drug beads, and solvent beads, respectively. The parameters were set according to the experimental conditions. The interaction parameter between the R blocks and the drug beads (a_{RD}) was set as 20. Since the rod blocks were solvophobic, the interaction parameter between R blocks and solvents (a_{RS}) was set to be 50.

3. Results and Discussion

The blank and drug-loaded micelles were prepared by a self-assembly method. First, the PEG-*g*-PBLG graft copolymers and DOX were separately dissolved in DMF, and mixed together with various DOX weight fractions (f_{DOX}). Then, water was slowly added to the PEG-*g*-PBLG/DOX mixture solutions under stirring. After dialyzing against water for 3 days, the aqueous solutions of the micelles were prepared.

The morphology of the micelles was observed by scanning electron microscopy (SEM) and transmission electron microscopy (TEM). As **Figure 1**a shows, the PEG-*g*-PBLG graft copolymers formed ellipse-like micelles. For the drug-loaded micelles, spherical shape was observed. Shown in Figure 1b is the morphology of the drug-loaded micelles formed with $f_{DOX} = 0.4$. TEM indicates the similar morphology of corresponding micelles (insets in Figure 1a,b). Dynamic light scattering (DLS) testing shows that the blank micelles have a

Table 2. Interaction parameters $a_{\alpha\beta}$ (in DPD units) used in the simulations.

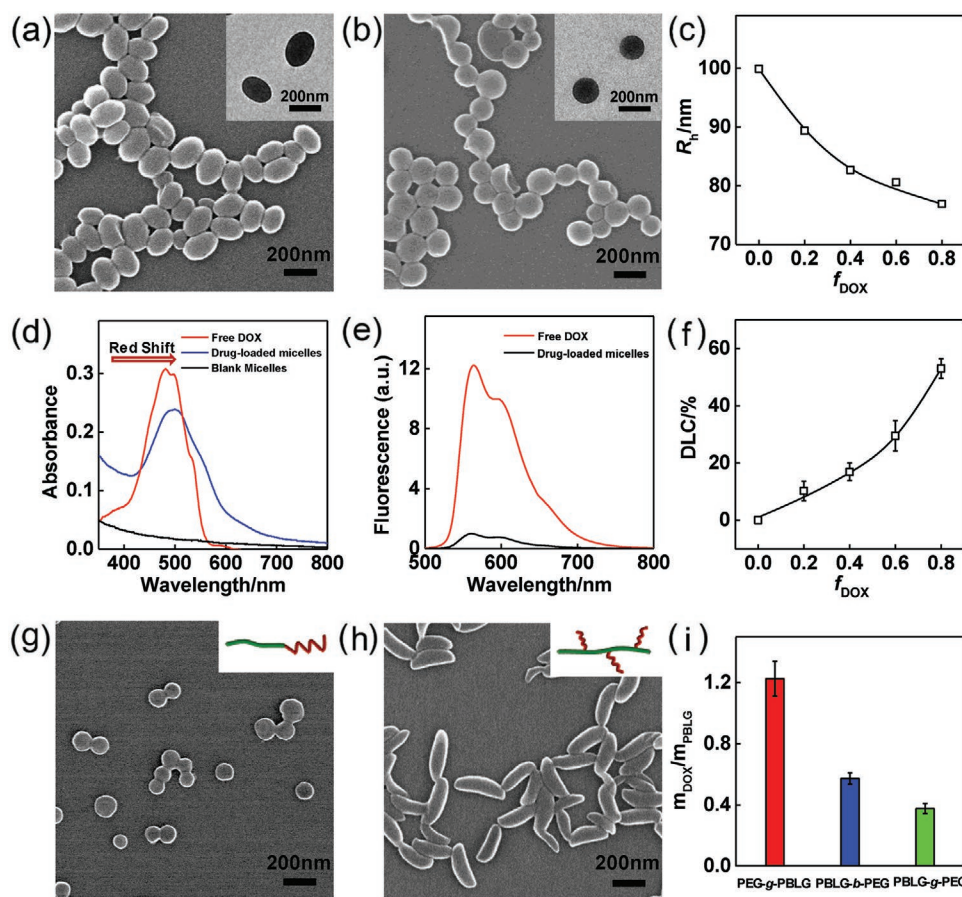|	R (PBLG)	C (PEG)	D (drug)	S (solvent)
R (PBLG)	25	50	20	50
C (PEG)	50	25	35	26
D (drug)	20	35	25	30
S (solvent)	50	26	30	25

2000121 (3 of 9)

Figure 1. a,b) SEM images of the PEG-*g*-PBLG blank micelles (a) and the PEG-*g*-PBLG/DOX drug-loaded micelles (b) (f_{DOX} = 0.4). Insets are corresponding TEM images. c) R_h values of the blank micelles and drug-loaded micelles (scattering angle 90°). d,e) UV–vis and fluorescence spectra of free DOX and the drug-loaded micelles. f) Plots of DLC of the micelles versus f_{DOX}. g,h) SEM images of blank micelles self-assembled from PBLG-*b*-PEG (g) and PBLG-*g*-PEG (h) copolymers. i) Plots of m_{DOX}/m_{PBLG} of the drug-loaded micelles (f_{DOX} = 0.8) versus copolymer topology.

hydrodynamic radius (R_h) of about 100 nm, and the R_h value decreases gradually with increasing f_{DOX} (for the drug-loaded micelles prepared with f_{DOX} = 0.8, R_h ≈ 77 nm). In addition, DLS testing reveals that all these micelles possess narrow size distributions (Figure S5, Supporting Information). Moreover, these drug-loaded micelles possess high stability in solution with no obvious morphology and size variation was observed after being stored for 1 month. However, for the drug-loaded micelles prepared with f_{DOX} > 0.8, they are less stable in solution and precipitates were observed in 1 week.

The loading of the DOX in the micelles is confirmed by the UV–vis and fluorescence spectra. As shown in Figure 1d, free DOX exhibit characteristic absorbance at 485 nm, and a pronounced red shift of the absorption peak from 485 to 500 nm is observed for drug-loaded micelles, which could ascribe to the formation of π–π stacking between DOX and PBLG segments.[21,30,31] The fluorescence intensity of free DOX is much greater than that of the drug-loaded micelles with corresponding DOX concentration. The fluorescence quenching of DOX in micelles (Figure 1e) should be caused by the formation of π–π stacking of DOX with PBLG segments.[17,21,30] From these testing, the loading of DOX in the micelles core and the existence of π–π stacking between DOX and PBLG segments are confirmed.

To determine the DLC of the micelles, 1 mL micelle solution was mixed with 4 mL DMF to break the micelles, and then the characteristic UV absorbance of DOX at 485 nm was compared with the standard curve generated from DOX solutions in H_2O/DMF (v/v, 1/4).[18,32,33] As shown in Figure 1f, the DLC increases gradually with increasing f_{DOX}. For example, at f_{DOX} = 0.4, the DLC is about 20%, and at f_{DOX} = 0.8, the DLC reaches 53.1%. Note that for DLC = 53.1%, the mass ratio of DOX to the polymer ($m_{DOX}/m_{polymer}$) is 1.14 (Figure S6, Supporting Information). These results clearly indicate an ultrahigh drug-loading capacity of the PEG-*g*-PBLG micelles comparing with common polymeric micelle systems. The high drug-loading capacity of the PEG-*g*-PBLG micelles should be related to the coil-*g*-rod topology of the graft copolymers. For these PEG-*g*-PBLG graft copolymers, the flexible PEG backbones form the shell and the rigid PBLG grafts form the core of the micelles. In the core region, the rigid PBLG grafts could distribute disorderly, which enables these graft copolymer micelles to achieve a high DLC.

To verify the effect of the copolymer topology on drug-loading capacity of the micelles, two copolymers composing of similar chemical composition with the PEG-*g*-PBLG graft copolymers, including PBLG-*b*-PEG block copolymers and

ADVANCED
SCIENCE NEWS
www.advancedsciencenews.com

Macromolecular
Chemistry and Physics
www.mcp-journal.de

PBLG-*g*-PEG graft copolymers, were synthesized. Details of the structure of the copolymers are presented in Supporting Information. The blank micelles and drug-loaded micelles were prepared in similar ways to those of the PEG-*g*-PBLG micelle systems. It was found that the PBLG-*b*-PEG self-assembled into spheres (Figure 1g), and the PBLG-*g*-PEG formed spindle-like micelles (Figure 1h). For the drug-loaded micelles, no evident morphological variation is observed comparing with corresponding blank micelles. The drug-loading capacity of these different micelles is compared at $f_{DOX} = 0.8$. To exclude the influence of PEG molecular weight, we use the mass ratio of DOX to PBLG (m_{DOX}/m_{PBLG}) to evaluate the drug-loading capacity of the micelles. As shown in Figure 1i, the PEG-*g*-PBLG copolymer micelles exhibit the highest drug-loading capacity ($m_{DOX}/m_{PBLG} = 1.23$), while PBLG-*g*-PEG copolymer micelles display the lowest ($m_{DOX}/m_{PBLG} = 0.38$).

Since the chemical compositions of these copolymers are similar, the significant differences in the DLC of these micelles should be attributed to the structure of the micelles, especially, the structure of the micelle core. As discussed above, the micelles formed by the PEG-*g*-PBLG graft copolymers possess a loose core due to the random distribution of the rigid PBLG grafts in the micelle core, which results in high drug-loading capacity. While for the PBLG-*g*-PEG graft copolymers, the rigid PBLG backbones prefer to pack in a side-by-side way, resulting in spindle-like micelles, in which DOX molecules are hardly encapsulated.[3,29,34,35] For the PBLG-*b*-PEG block copolymers, although they prefer to take ordered packing, the formed micelles usually possess a relatively loose structure due to the repulsive interactions among PEG chains.[36,37] As a result, the PBLG-*b*-PEG micelles have a relatively higher drug-loading capacity comparing with PBLG-*g*-PEG micelles.

From the experiments, the detailed structures such as distribution of drugs and the packing of polymer chains are hard to be obtained.[38] Therefore, it is difficult to get a deep understanding of the effect of structural difference of the micelles on drug-loading capacity. To address these issues, DPD simulations on model systems were performed.[32,39,40] According to the experiment studies, coarse-grained models of coil-*g*-rod graft copolymers (C_{12}-*g*-$(R_6)_4$), rod-*b*-coil block copolymers (R_{12}-*b*-C_6), and rod-*g*-coil graft copolymers (R_{12}-*g*-$(C_2)_3$), as well as the drug molecule (D) were constructed (**Figure 2**a). The hydrophobic rigid R segments represent the PBLG segments, and the hydrophilic flexible C segments represent the PEG segments. The rigidity of the R segments is achieved by a harmonic angle potential.[41] The repulsive interaction parameter between the same type of beads ($a_{\alpha\alpha}$) was set as 25, and the repulsive interaction parameter between the R blocks and D beads (a_{RD}) was set as 20 (note: smaller repulsion corresponds to stronger attraction in the simulation). Details of the DPD method and parameter settings can be found in Supporting Information.

As shown in Figure 2b–d, the C-*g*-R model graft copolymers, the R-*b*-C model block copolymers, and R-*g*-C model graft copolymers self-assemble into ellipse-like, spherical, and spindle-like core–shell micelles, respectively. In these micelles, the rigid hydrophobic R segments form the core and the flexible hydrophilic C segments form the shell. For the model polymer/drug

mixtures, spherical micelles (C-*g*-R/Drug mixtures and R-*b*-C/Drug mixtures) or spindle-like micelles (R-*g*-C/Drug mixtures) were obtained (Figure 2e–g). As shown in Figure 2h, the C-*g*-R micelles exhibit the highest m_{Drug}/m_{Rod} value, while the m_{Drug}/m_{Rod} value of the R-*g*-C micelles is the lowest, which is well consistent with experimental results.

To evaluate the structural difference of these micelles formed by different copolymers, the orientation order parameter, a quantitative measure for the degree of ordered packing of rod blocks in the micelles, was calculated.[42] As shown in Figure 2i, the orientation order parameter of R rods from the R-*g*-C is highest (about 0.79), and that from the C-*g*-R is lowest (about 0.60). The orientation order parameter results and snapshots of micelles indicate that the rod segments of C-*g*-R copolymers pack in a less ordered mode and lead to a looser core, which provides space for encapsulation of drugs and results in higher drug-loading capacity; while for the R-*g*-C copolymers, the rod segments align along the long axis of spindle-like micelles in a side-by-side way leaving small room in the core, which hinders encapsulating drugs. These DPD simulations well reproduced the experiment results, and confirmed that the high drug-loading capacity of PEG-*g*-PBLG micelles is benefited from their special molecular packing mode.

To further illustrate how the PBLG blocks and the drugs cooperatively form the core, we also plotted the density profiles of R blocks and drug models from the simulation results. As shown in **Figure 3**a, for the drug-loaded micelles formed by C-*g*-R/Drug mixtures, there are one peak for the drugs and one valley for the rigid blocks in the center of micelles. On the contrary, for the R-*b*-C/Drug (Figure 3b) and R-*g*-C/Drug (Figure 3c) micelles, there are one valley for the drugs and one peak for the rigid blocks in the center. These results further confirm that the C-*g*-R copolymers packs much looser in the center than the R-*b*-C and R-*g*-C copolymers, which contributes to the higher drug loading.

In addition to the topology of the copolymers, the effect of structure characters of the PEG-*g*-PBLG graft copolymers, including the length of the PBLG side chain, the length of the PEG backbone, and the grafting ratio of the PBLG side chains on the drug-loading capacity of the micelles are also studied by experiments and simulations (**Figure 4**). Shown in Figure 4a is the m_{DOX}/m_{PBLG} values of the micelles self-assembled from graft copolymers with various lengths of PBLG grafts, that is, PEG$_{110}$-*g*-(PBLG$_{13}$)$_{11}$, PEG$_{110}$-*g*-(PBLG$_{28}$)$_{11}$, and PEG$_{110}$-*g*-(PBLG$_{61}$)$_{11}$. It was found that an increase in the length of PBLG side chain results in a slight decrease in drug-loading capacity of micelles. In DPD simulations, C-*g*-R model graft copolymers with various lengths of side chains were constructed (including C_{12}-*g*-$(R_4)_4$, C_{12}-*g*-$(R_6)_4$, and C_{12}-*g*-$(R_8)_4$) and the drug-loading capacity of the micelles self-assembled from these model graft copolymers was studied. As can be seen from Figure 4b, with increasing the length of the side chain from 4 to 8, the value of m_{Drug}/m_{Rod} is gradually decreased. Such a result is consistent with the experimental observations. In addition, the orientation order parameter of R rods in the micelles is analyzed (Figure 4b). The orientation order parameter of R rods from the C_{12}-*g*-$(R_4)_4$ is lowest (about 0.58), and that from C_{12}-*g*-$(R_8)_4$ is highest (about 0.64), which correspond to the conclusion

ADVANCED
SCIENCE NEWS
www.advancedsciencenews.com

Macromolecular
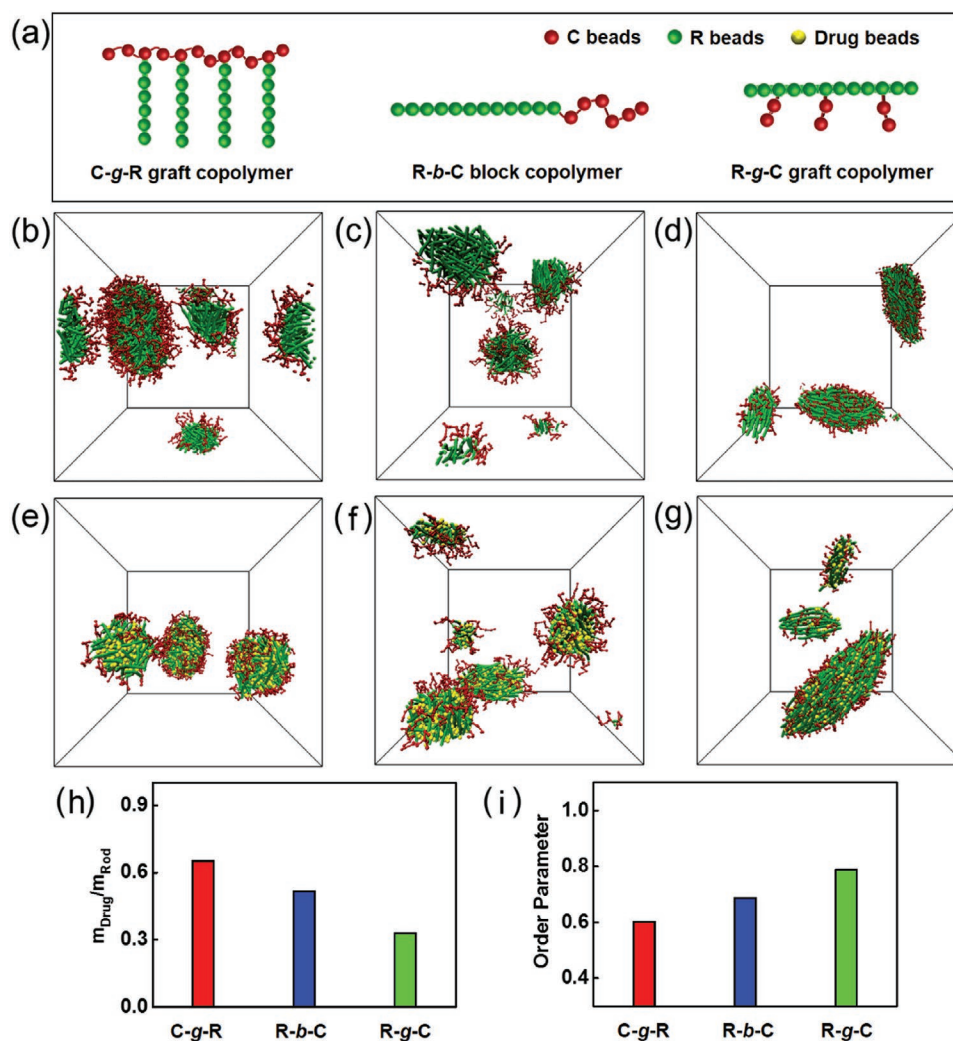**Chemistry and Physics**
www.mcp-journal.de

Figure 2. a) DPD models of C-*g*-R, R-*b*-C, R-*g*-C copolymers, and drug molecules. b–d) Simulation snapshots of blank micelles self-assembled from C-*g*-R, R-*b*-C, and R-*g*-C model copolymers, respectively. e–g) Simulation snapshots of drug-loaded micelles self-assembled from C-*g*-R/Drug, R-*b*-C/Drug, and R-*g*-C/Drug mixtures, respectively. h) Plots of m_{Drug}/m_{Rod} of the drug-loaded micelles versus topology of the model copolymers ($f_{Drug} = 0.8$). i) Order parameter of rod segments in the micelles versus topology of the model copolymers ($f_{Drug} = 0.8$).

we proposed that a more ordered packing of rod segments in micelle cores results in a lower drug-loading capacity of the micelles.

The influence of the length of PEG backbone and the grafting ratio on drug-loading capacity were also evaluated. Since only one kind of PEG-*g*-NH$_2$ initiator (the DP of the PEG backbone is 110, and the substitution number of the amino groups is 11) was obtained, the influence of the length of PEG backbone and the grafting ratio cannot be studied experimentally. Therefore, DPD simulations were performed on model systems with various backbone length and grafting ratios. It was found that with increasing the length of PEG backbone from 9 to 15 (Figure 4c), or with decreasing the grafting ratio from 1/3 to 1/6 (Figure 4d), the drug-loading capacity of micelles (m_{Drug}/m_{Rod}) decreases. Simultaneously, with such structural changes in the copolymers, the orientation order parameter of R rods in micelle cores slightly increases, which hinders micelles from encapsulating more model drugs. From

these experiments and simulations, we can conclude that: 1) the low ordering of rod blocks facilitates the encapsulation of drugs, while the high ordering of rod blocks hinders the encapsulation of drugs; 2) the higher ordering of the rod blocks in micelle core can be achieved by these coil-*g*-rod graft copolymers with lower grafting ratios, longer backbones, or longer side chains.

The strong π–π stacking interaction between DOX and core-forming PBLG chains is also found to be an important factor contributing to the high DLCs of the PEG-*g*-PBLG micelles. When the benzyl groups on PBLG side chains were partially substituted by ethyl groups, the π–π stacking interaction between DOX and polymers was weakened;[43] as a result, drug loading capacity was weakened. Four PEG-*g*-P(BLG-*co*-ELG) (P(BLG-*co*-ELG):poly((γ-benzyl-co-γ-ethyl)-L-glutamate)) copolymers with different degree of substitution (DS) were synthesized and studied in this work. As shown in **Figure 5**a, the $m_{DOX}/m_{polypeptide}$ (the subscript "polypeptide" denotes
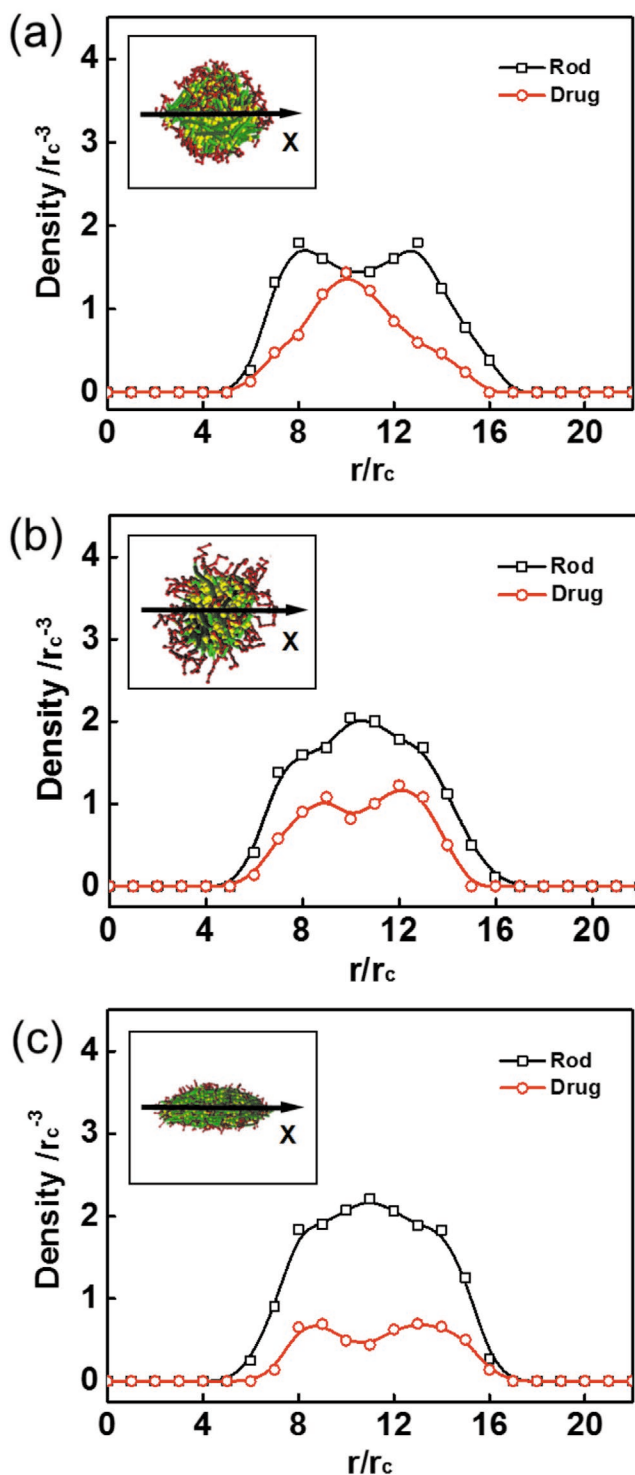
**ADVANCED
SCIENCE NEWS**
www.advancedsciencenews.com

**Macromolecular
Chemistry and Physics**
www.mcp-journal.de

Figure 3. The density profiles of the drug-loaded micelles self-assembled from a) C-*g*-R/Drug, b) R-*b*-C/Drug, and c) R-*g*-C/Drug mixtures. Insets are corresponding micelles marked with arrows.

both the PBLG and the P(BLG-*co*-ELG) segments) decreases gradually from 1.23 to 0.72 with increasing the DS from 0% to

37%. Such a trend was further investigated by simulations. In the simulations, to model the effect of substitution of benzyl groups by ethyl groups, the R beads in the rod segments were randomly replaced by M beads, and the repulsive interaction parameter between M beads and drug (a_{MD}) was set as 35, representing weaker attraction between M and D beads than that between R and D beads ($a_{RD} = 20$). Figure 5b shows the plots of m_{Drug}/m_{Rod} value as a function of DS. As can be seen, the m_{Drug}/m_{Rod} decreases with increasing DS, while the order parameter of the rod segments remains unchanged (inset of Figure 5b). These results revealed the influence of interaction between core-forming polymers and drugs on drug-loading capacity of the micelles. Note that the $m_{DOX}/m_{polypeptide}$ values are still on a high level for all these micelles.

As reported in literature, in most cases, the DLC of polymeric micelle systems is on the level of 10 wt%. It is a challenge to achieve high drug-loading contents in convenient ways.[18,19] In this work, as revealed by the experiment and simulation studies, by the co-assembly of coil-*g*-rod copolymers and DOX model drugs, micellar systems with an ultra-high drug-loading capacity (up to 53.1 wt%) can be prepared. The coil-*g*-rod topology of the copolymers is critical to achieve such high drug-loading capacity. The results presented in this work may provide new ideas for improving drug-loading capacity of polymeric micelles.

Finally, bio-related properties of the drug-loaded micelles derived from PEG-*g*-PBLG graft copolymers, including in vitro biocompatibility and drug release behaviors, were studied (**Figure 6**). The biocompatibility of the drug-loaded micelles was evaluated against NIH/3T3 cells by the tetrazolium salt (MTT) assay.[22,31,44] For the blank micelles, due to the good biocompatibility of the PEG and polypeptide blocks,[14–16] no obvious cytotoxicity was observed after being incubated for 48 h with the polymer concentration up to 300 µg mL^{-1} (Figure S9, Supporting Information). As shown in Figure 6a, both the free DOX and drug-loaded micelles display dose-dependent cytotoxicity, while the drug-loaded micelles are less cytotoxic than free DOX. Taking the group with equivalent DOX concentration of 0.2 µg mL^{-1}, for example, about 50% cellular growth is inhibited by the free DOX trial, while for the drug-loaded micelles, a higher cell viability of 85% is observed.

The in vitro release profile of DOX from the drug-loaded micelles is presented in Figure 6b. Rapid release is observed in the initial stage and followed by slow and sustained release. Moreover, the release behavior is pH-relative. Faster release is achieved at pH 5.5. The total release amount in 96 h increases from about 42% to about 62% when the pH value decreases from 7.4 to 5.5. The pH-relative release behavior could be attributed to the increase of solubility of DOX in acidic condition due to the increased protonation of amine group.[18,22,45] The pH-relative release behavior will benefit the accelerated drug release in tumor site.[46]

4. Conclusion

In summary, we report that micelles self-assembled from PEG-*g*-PBLG coil-*g*-rod graft copolymers display a high DOX-loading content. The structure of the drug-loaded micelles was
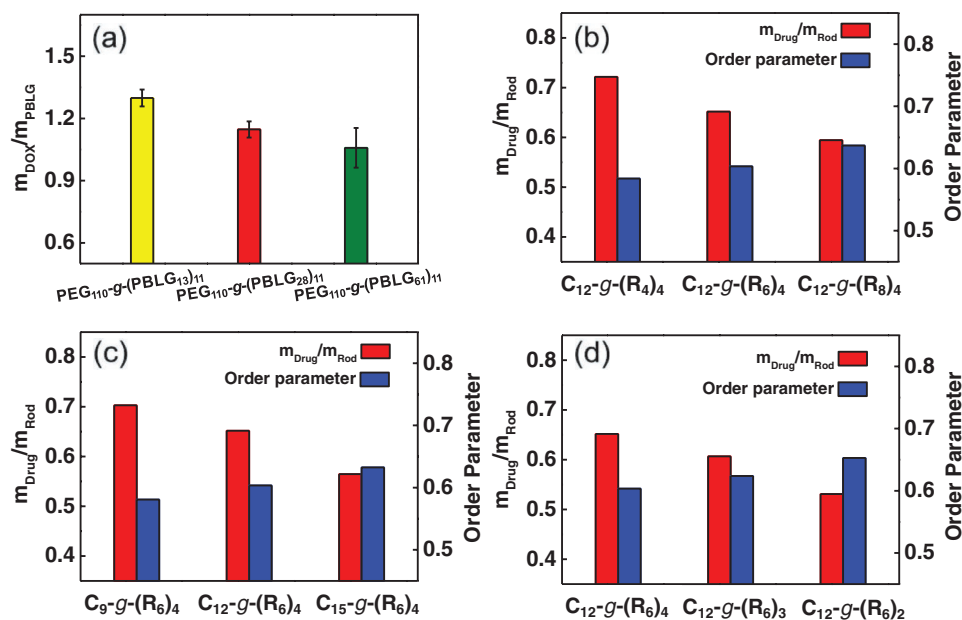
Figure 4. a) Plots of m_{DOX}/m_{PBLG} of the drug-loaded micelles self-assembled from PEG-g-PBLG copolymers with various PBLG side chain lengths ($f_{DOX} = 0.8$). b–d) The plots of m_{Drug}/m_{Rod} values of drug-loaded micelles and order parameter of rod segments in micelle cores as functions of b) the length of rod side chains, c) the length of backbone, and d) the grafting ratio of side chains obtained from DPD simulations. ($f_{Drug} = 0.8$).
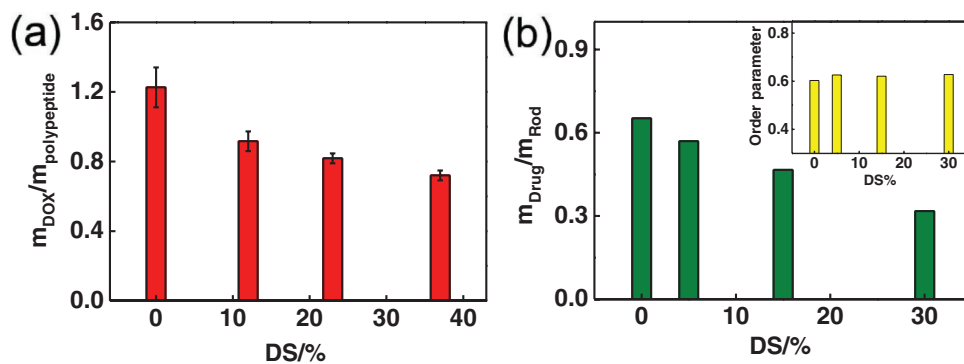

Figure 5. a) Plots of $m_{DOX}/m_{polypeptide}$ of the drug-loaded micelles self-assembled from PEG-g-P(BLG-co-ELG) copolymers with various DS ($f_{DOX} = 0.8$); b) simulations for the m_{Drug}/m_{Rod} of drug-loaded micelles self-assembled from C-g-(R-co-M) model copolymers with various DS ($f_{Drug} = 0.8$). Inset in (b) shows order parameters of rod blocks in the drug-loaded micelles.
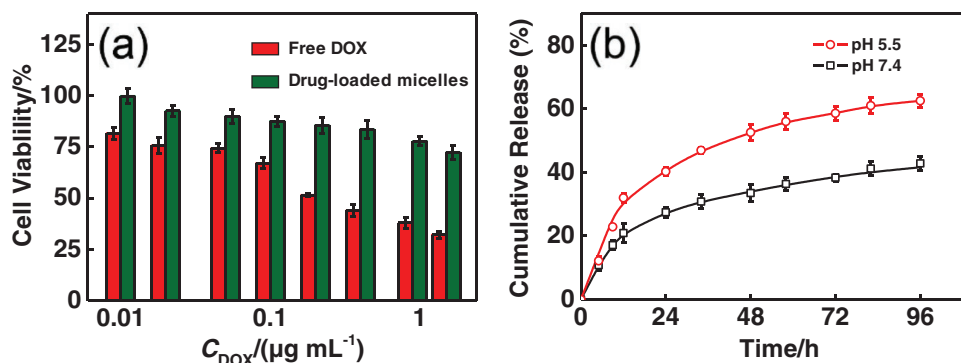

Figure 6. a) In vitro cytotoxicity studies of free DOX and PEG-g-PBLG/DOX micelles against NIH/3T3 cells after 48 h incubation. b) In vitro DOX release profiles of PEG-g-PBLG/DOX micelles (DLC = 53.1%) at pH 7.4 and pH 5.5.

explicated by the combination of experiments and simulations. The loose core of the micelles induced by coil-*g*-rod topology of the polymers as well as the strong attraction between PBLG grafts and DOX contributes to the high drug-loading capacity. The cytotoxicity of DOX against model cells was decreased after being loaded in the micelles, and the DOX released from the micelles sustainably. This work indicates that micelles with a loose core could serve as vehicles with high-loading capacities, and the coil-*g*-rod graft copolymers are effective building blocks toward micelles with a loose core.

Supporting Information

Supporting Information is available from the Wiley Online Library or from the author.

Conflict of Interest

The authors declare no conflict of interest.

[1] C. Feng, Y. Li, D. Yang, J. Hu, X. Zhang, X. Huang, *Chem. Soc. Rev.* **2011**, *40*, 1282.

[2] C. Cai, J. Lin, Y. Lu, Q. Zhang, L. Wang, *Chem. Soc. Rev.* **2016**, *45*, 5985.

[3] C. Yang, L. Gao, J. Lin, L. Wang, C. Cai, Y. Wei, Z. Li, *Angew. Chem., Int. Ed.* **2017**, *56*, 5546.

[4] B. Xu, C. Feng, X. Huang, *Nat. Commun.* **2017**, *8*, 333.

[5] D. Tao, C. Feng, Y. Cui, X. Yang, I. Manners, M. A. Winnik, X. Huang, *J. Am. Chem. Soc.* **2017**, *139*, 7136.

[6] J. Tan, D. Chong, Y. Zhou, R. Wang, X. Wan, J. Zhang, *Langmuir* **2018**, *34*, 8975.

[7] H. Cabral, K. Miyata, K. Osada, K. Kataoka, *Chem. Rev.* **2018**, *118*, 6844.

[8] Y. Que, Y. Liu, W. Tan, C. Feng, P. Shi, Y. Li, H. Xiaoyu, *ACS Macro Lett.* **2016**, *5*, 168.

[9] H. Chen, Z. Gu, H. An, C. Chen, J. Chen, R. Cui, S. Chen, W. Chen, X. Chen, X. Chen, Z. Chen, B. Ding, Q. Dong, Q. Fan, T. Fu, D. Hou, Q. Jiang, H. Ke, X. Jiang, G. Liu, S. Li, T. Li, Z. Liu, G. Nie, M. Ovais, D. Pang, N. Qiu, Y. Shen, H. Tian, C. Wang, et al. *Sci. China: Chem.* **2018**, *61*, 1503.

[10] P. Wang, N. Yu, Y. Wang, H. Sun, Z. Yang, S. Zhou, *J. Mater. Chem. B* **2018**, *6*, 112.

[11] J. Lin, J. Zhu, T. Chen, S. Lin, C. Cai, L. Zhang, Y. Zhuang, X.-S. Wang, *Biomaterials* **2009**, *30*, 108.

[12] M. Xu, C. Y. Zhang, J. Wu, H. Zhou, R. Bai, Z. Shen, F. Deng, Y. Liu, J. Liu, *ACS Appl. Mater. Interfaces* **2019**, *11*, 5701.

[13] C. Feng, X. Huang, *Acc. Chem. Res.* **2018**, *51*, 2314.

[14] C. He, X. Zhuang, Z. Tang, H. Tian, X. Chen, *Adv. Healthcare Mater.* **2012**, *1*, 48.

[15] C. Deng, J. Wu, R. Cheng, F. Meng, H.-A. Klok, Z. Zhong, *Prog. Polym. Sci.* **2014**, *39*, 330.

[16] Z. Song, Z. Han, S. Lv, C. Chen, L. Chen, L. Yin, J. Cheng, *Chem. Soc. Rev.* **2017**, *46*, 6570.

[17] K. Liang, J. E. Chung, S. J. Gao, N. Yongvongsoontorn, M. Kurisawa, *Adv. Mater.* **2018**, *30*, 1706963.

[18] C. Sanson, C. Schatz, J.-F. Le Meins, A. Soum, J. Thévenot, E. Garanger, S. Lecommandoux, *J. Controlled Release* **2010**, *147*, 428.

[19] S. Lv, Y. Wu, K. Cai, H. He, Y. Li, M. Lan, X. Chen, J. Cheng, L. Yin, *J. Am. Chem. Soc.* **2018**, *140*, 1235.

[20] S. S. Dunn, J. C. Luft, M. C. Parrott, *Nanoscale* **2019**, *11*, 1847.

[21] Z. Liu, X. Sun, N. Nakayama-Ratchford, H. Dai, *ACS Nano* **2007**, *1*, 50.

[22] C. Yang, A. B. Ebrahim Attia, J. P. K. Tan, X. Ke, S. Gao, J. L. Hedrick, Y.-Y. Yang, *Biomaterials* **2012**, *33*, 2971.

[23] S. Lv, Z. Tang, M. Li, J. Lin, W. Song, H. Liu, Y. Huang, Y. Zhang, X. Chen, *Biomaterials* **2014**, *35*, 6118.

[24] B. Xia, B. Wang, W. Zhang, J. Shi, *RSC Adv.* **2015**, *5*, 44660.

[25] Y. Tang, R. Mei, S. Yang, H. Tang, W. Yin, Y. Xu, Y. Gao, *Superlattices Microstruct.* **2016**, *92*, 256.

[26] S. Xu, J. Shi, D. Feng, L. Yang, S. Cao, *J. Mater. Chem. B* **2014**, *2*, 6500.

[27] Y. Wang, Y. Yan, J. Cui, L. Hosta-Rigau, J. K. Heath, E. C. Nice, F. Caruso, *Adv. Mater.* **2010**, *22*, 4293.

[28] E. R. Blout, R. H. Karlson, *J. Am. Chem. Soc.* **1956**, *78*, 941.

[29] C. Cai, J. Lin, T. Chen, X. Tian, *Langmuir* **2010**, *26*, 2791.

[30] Y. Liang, X. Deng, L. Zhang, X. Peng, W. Gao, J. Cao, Z. Gu, B. He, *Biomaterials* **2015**, *71*, 1.

[31] X. Gu, M. Qiu, H. Sun, J. Zhang, L. Cheng, C. Deng, Z. Zhong, *Biomater. Sci.* **2018**, *6*, 1526.

[32] L. Chen, T. Jiang, C. Cai, L. Wang, J. Lin, X. Cao, *Adv. Healthcare Mater.* **2014**, *3*, 1508.

[33] Y. Lili, M. Ruihua, L. Li, L. Fei, Y. Lin, S. Li, *Int. J. Pharm.* **2016**, *498*, 195.

[34] H. Gao, X. Ma, J. Lin, L. Wang, C. Cai, L. Zhang, X. Tian, *Macromolecules* **2019**, *52*, 7731.

[35] Z. Zhuang, T. Jiang, J. Lin, L. Gao, C. Yang, L. Wang, C. Cai, *Angew. Chem., Int. Ed.* **2016**, *55*, 12522.

[36] C. Cai, L. Wang, J. Lin, X. Zhang, *Langmuir* **2012**, *28*, 4515.

[37] C. Cai, L. Wang, J. Lin, *Chem. Commun.* **2011**, *47*, 11189.

[38] Z. Zhuang, X. Zhu, C. Cai, J. Lin, L. Wang, *J. Phys. Chem. B* **2012**, *116*, 10125.

[39] Z. Xu, J. Lin, Q. Zhang, L. Wang, X. Tian, *Polym. Chem.* **2016**, *7*, 3783.

[40] Q. Zhang, J. Lin, L. Wang, Z. Xu, *Prog. Polym. Sci.* **2017**, *75*, 1.

[41] W. Xu, Z. Xu, C. Cai, J. Lin, S. Zhang, L. Zhang, S. Lin, Y. Yao, H. Qi, *J. Phys. Chem. Lett.* **2019**, *10*, 6375.

[42] K. E. Polovnikov, I. I. Potemkin, *J. Phys. Chem. B* **2017**, *121*, 10180.

[43] Z. Zhuang, C. Cai, T. Jiang, J. Lin, C. Yang, *Polymer* **2014**, *55*, 602.

[44] D. Kakkar, S. Mazzaferro, J. Thevenot, C. Schatz, A. Bhatt, B. S. Dwarakanath, H. Singh, A. K. Mishra, S. Lecommandoux, *Macromol. Biosci.* **2015**, *15*, 124.

[45] C. Zheng, L. Qiu, X. Yao, K. Zhu, *Int. J. Pharm.* **2009**, *373*, 133.

[46] S. Lv, M. Li, Z. Tang, W. Song, H. Sun, H. Liu, X. Chen, *Acta Biomater.* **2013**, *9*, 9330.